https://doi.org/10.5194/egusphere-2026-4358
Preprint. Discussion started: 29 July 2026
© Author(s) 2026. CC BY 4.0 License.

Validation of ATLID stratospheric aerosol retrievals using SAGE III/ISS and ground-based lidar observations

Eddy A. Poncet[1,2], Sergey M. Khaykin[1], Sophie Godin-Beekmann[1], and Thierry Leblanc[3]

[1]LATMOS/IPSL, CNRS, UVSQ Université Paris-Saclay, Sorbonne Université, Guyancourt, France
[2]École Centrale de Lyon / Université Claude Bernard Lyon 1, France
[3]Jet Propulsion Laboratory, California Institute of Technology, Wrightwood, CA, USA

Correspondence: Sergey M. Khaykin (sergey.khaykin@latmos.ipsl.fr)

Abstract. We present a systematic validation of EarthCARE ATLID stratospheric aerosol retrievals against SAGE III/ISS and ground-based lidars at the Table Mountain Facility (TMF) and the Observatoire de Haute-Provence (OHP), using 895 SAGE III/ISS, 55 TMF, and 26 OHP collocations over August 2024-April 2026 and spanning background, volcanic, and wildfire smoke conditions. We evaluate a Level-1-based extinction product, derived directly from the ATLID L1 scattering ratio. Against SAGE III/ISS, this L1 product yields a regression slope of 1.04 for the stratospheric aerosol optical depth (sAOD) and an overall median relative extinction difference of $-2.3\,\%$; across all matchups, the relative sAOD bias has a global mean of $-3.2\,\%$ with a standard deviation of $65.7\,\%$. The altitude-resolved comparison reveals a moderate positive bias near the tropopause ($\sim +10\,\%$), a pronounced negative excursion of up to $-15\,\%$ in the lower-to-mid stratosphere, and convergence toward near-zero bias above ∼25 km, together with a systematic negative sAOD bias in the Northern Hemisphere extratropics that increases with latitude. Independent backscatter comparisons against TMF and OHP reproduce the same negative bias in the lower-to-mid stratosphere (median differences of $-5.5\,\%$ and $-10.6\,\%$, respectively), indicating that this feature originates in the Level-1 scattering-ratio retrieval itself rather than in the extinction-conversion step. Daytime collocations are markedly noisier than nighttime ones (relative-difference standard deviation of ∼32 % versus ∼17 %), although the median bias remains close to zero in both cases. In contrast, the native L2 product achieves a regression slope of only 0.64 against SAGE III/ISS sAOD, largely driven by frequent null retrievals under low-aerosol conditions. Even when excluding these missed detections, the correlation remains weak ($R = 0.26$), and the L2 product systematically overestimates peak extinction in dense plumes, making it unreliable for stratospheric monitoring in its current processing baseline.

1 Introduction

The EarthCARE satellite mission, launched on 28 May 2024 as part of a collaboration between ESA (European Space Agency) and JAXA (Japan Aerospace Exploration Agency), carries four co-aligned instruments designed to characterize clouds, aerosols, and radiation from space (Wehr et al., 2023). Among these, the Atmospheric Lidar (ATLID) operates at 355 nm and provides vertically resolved profiles of aerosol backscatter, extinction, and depolarization ratio with an unprecedented combination of sensitivity and global coverage (ESA Earth Online, 2026). ATLID's high-spectral-resolution lidar (HSRL) capability allows the independent retrieval of the backscatter and extinction coefficients without prior assumptions

https://doi.org/10.5194/egusphere-2026-4358
Preprint. Discussion started: 29 July 2026
© Author(s) 2026. CC BY 4.0 License.

on the lidar ratio, representing a significant advancement over conventional elastic-backscatter lidars (van Zadelhoff et al., 2024).

Stratospheric aerosols play a well-recognized role in climate variability and ozone chemistry, modulating the Earth's radiative budget and providing surfaces for heterogeneous chemical reactions (Kremser et al., 2016). Long-term monitoring of the stratospheric aerosol layer requires accurate, well-characterized observations from multiple platforms. Ground-based lidar networks such as NDACC (Network for the Detection of Atmospheric Composition Changes) provide continuous vertically resolved measurements at fixed locations (NDACC, 2026), while solar occultation instruments aboard satellites, most notably the Stratospheric Aerosol and Gas Experiment (SAGE) series, have historically provided the backbone of global stratospheric aerosol climatologies (Thomason et al., 2023). The SAGE III instrument aboard the International Space Station (SAGE III/ISS), operational since 2017, continues this legacy by delivering high-quality extinction profiles at multiple wavelengths, from which 355 nm extinction can be derived.

The validation of ATLID stratospheric aerosol retrievals is a critical step before the data can be used for scientific applications. Complementary case-study validations of the operational ATLID Level-2 aerosol profiling products against ground-based lidars have recently been reported in the troposphere (Baars et al., 2026), whereas a systematic assessment in the stratosphere (the focus of the present study) is still lacking. This is particularly challenging in background conditions, where the aerosol signal is weak compared to molecular scattering. To address these challenges and thoroughly assess the official Level-2 (L2) performance, an alternative approach based on Level-1 backscatter signals and Rayleigh backscatter from meteorological data, described in Khaykin et al. (2026), is utilized to allow robust extinction retrieval even under low-aerosol conditions.

The study period (August 2024 - April 2026) encompasses a diverse range of atmospheric conditions in the stratosphere, including background aerosol, the volcanic plume from the eruption of Ruang volcano (Indonesia) in April-May 2024 (Khaykin et al., 2026), and intense wildfire smoke injections into the lower stratosphere during the boreal summer of 2025 (Haarig et al., 2026). This variety offers a unique opportunity to assess ATLID's performance across contrasting aerosol regimes and to identify potential sources of systematic discrepancy between ATLID and independent observations.

In this paper, we present a systematic comparison of ATLID-derived stratospheric aerosol extinction and scattering ratio profiles with collocated SAGE III/ISS observations and ground-based lidar measurements from the Table Mountain Facility (TMF, California) and the Observatoire de Haute-Provence (OHP, France). We characterize the absolute and relative bias between ATLID and the reference instruments as a function of altitude, latitude, season, and aerosol loading, and we discuss the potential origins of observed discrepancies. The paper is organized as follows. Section 2 describes the instruments and data used in this study, the collocation methodology, and the comparison metrics. Section 3 presents the comparison results. Section 4 discusses the sources of the observed bias. Section 5 provides the conclusions.

https://doi.org/10.5194/egusphere-2026-4358
Preprint. Discussion started: 29 July 2026
© Author(s) 2026. CC BY 4.0 License.

2 Data and Methods

2.1 The EarthCARE mission and ATLID instrument

Detailed descriptions of the EarthCARE mission and the ATLID instrument are provided by Wehr et al. (2023) and ESA Earth Online (2026); here we summarise only the characteristics relevant to the present study. EarthCARE orbits at approximately 393 km altitude in a sun-synchronous orbit with a 25-day repeat cycle. ATLID provides vertically resolved profiles of aerosol scattering ratio, backscatter, extinction, and linear depolarisation ratio with a vertical resolution of approximately 100 m below 20 km and 500 m above, and a nominal along-track horizontal resolution of approximately 285 m for single shots. For all ATLID products used in this study, we relied on baseline BA and its successors BB and BC.

2.2 ATLID Level-1 extinction retrieval

The official ATLID Level-2 (L2) product provides aerosol extinction profiles derived from the HSRL (Donovan et al., 2024). However, as suggested by Khaykin et al. (2026) (hereafter K26) and confirmed in this study, the L2 processor frequently fails to produce valid stratospheric retrievals under low-aerosol background conditions, defaulting to fill values in the absence of a sufficiently strong aerosol signal. In contrast, the L2 algorithm successfully retrieves extinction for optically thicker layers such as volcanic plumes. To overcome this limitation and enable a systematic comparison across all aerosol regimes, we derive ATLID aerosol extinction directly from the Level-1 scattering ratio (SR) using the K26 method. This method retrieves the unattenuated particulate backscatter coefficient β_{aer} from the molecular reference profile, which is itself computed from ECMWF meteorological profiles provided with the Level-2 data and interpolated onto the ATLID vertical grid. The aerosol extinction coefficient α_{aer} is then obtained as:

$$\alpha_{\mathrm{aer}}(z) = S_{\mathrm{aer}} \cdot \beta_{\mathrm{aer}}(z), \quad (1)$$

where S_{aer} is the lidar ratio. Because this derivation relies entirely on non-attenuated inputs derived from the molecular signal, the resulting extinction profiles are free from cumulative attenuation errors inherent to elastic-backscatter lidar inversions, though they remain sensitive to the lidar ratio.

The aerosol extinction coefficient is derived from the ATLID L1 particulate backscatter coefficient using Eq. (1). Wherever the ATLID L2 lidar ratio is available and falls within physically realistic bounds (30-90 sr), it is used directly in the retrieval. In all other cases, including profiles for which the L2 processor returns fill values or unphysical estimates, a constant fallback value of 50 sr is applied, consistent with values reported in the literature for aged stratospheric sulfate aerosols (Kremser et al., 2016). The sensitivity of the retrieved extinction to the lidar ratio, and in particular the impact of using a spatially variable L2 lidar ratio versus the fixed fallback, is discussed in Sect. 4.

Individual ATLID Level-1 profiles within each collocation window (see Sect. 2.5) are averaged to reduce random noise, and a 3-point boxcar smoothing is applied in the vertical dimension to the resulting mean profile. This smoothing improves the signal-to-noise ratio at stratospheric altitudes without significantly degrading the vertical resolution relevant to the features of interest.

https://doi.org/10.5194/egusphere-2026-4358
Preprint. Discussion started: 29 July 2026
© Author(s) 2026. CC BY 4.0 License.

2.3 SAGE III/ISS

The Stratospheric Aerosol and Gas Experiment III aboard the International Space Station (SAGE III/ISS) has been operational since June 2017 (Cisewski et al., 2014). It measures solar and lunar occultation spectra to retrieve vertically resolved profiles of aerosol extinction, ozone, water vapour, and other trace gases (Thomason et al., 2023). The solar occultation technique provides self-calibrating, high-accuracy measurements with a vertical resolution of approximately 0.5 km. SAGE III/ISS delivers approximately 30-40 solar occultation profiles per day, distributed across two latitude bands that precess over time due to the ISS orbital inclination.

In this study, we use SAGE III/ISS Version 6 aerosol extinction profiles at 355 nm, derived from the 384 nm channel and converted to 355 nm using the Ångström exponent computed from the 384-521 nm wavelength pair, for the period August 2024-April 2026. Prior to use, profiles were screened following the quality-control (QC) recommendations provided with the Level-2 product. Occultations affected by event-level anomalies, including pointing, blockage, timing, thermal-control, or ephemeris issues, were excluded, as were altitude bins flagged for signal disturbance or interpolation artefacts. For the aerosol comparisons, only measurements classified as background, perturbed, or enhanced aerosol by the SAGE aerosol classification flag were retained; profiles flagged as transmission anomalies, aerosol-cloud mixtures, or polar stratospheric clouds were discarded. Finally, only positive extinction values with a relative uncertainty below 50 % were retained in the point-by-point comparison with ATLID. SAGE III/ISS constitutes the primary reference instrument for this validation study owing to its high measurement accuracy, self-calibrating nature, and the large number of collocations achievable with ATLID over the study period.

2.4 Ground-based lidar instruments

2.4.1 Table Mountain Facility (TMF)

The JPL (Jet Propulsion Laboratory) Table Mountain Facility (TMF; Leblanc et al. 2012; 34.38° N, 117.68° W, 2285 m a.s.l.) in California hosts the TMSOL (Table Mountain Stratospheric Ozone Lidar), operated by NASA's Jet Propulsion Laboratory within the NDACC network. Aerosol profiles are derived from nighttime-only, high-intensity UV Rayleigh (355 nm) and Raman (387 nm) lidar returns measured two to five times per week. The data are processed using the NDACC-compliant Global Lidar Analysis Software Suite (GLASS) v1 algorithm (Leblanc et al., 2016a, b), yielding aerosol backscatter and scattering ratio profiles at 355 nm normalised in an aerosol-free reference region between 32 and 36 km. The total uncertainty on the retrieved profiles is approximately 10 % throughout most of the stratosphere, with a vertical resolution ranging from a few tens of metres in the lowermost stratosphere to about 2.5 km in the upper stratosphere (Khaykin et al., 2026).

In this study, we use the standard NDACC aerosol backscatter coefficient product at 355 nm, screened according to the associated quality flags and averaged onto 2 km altitude layers. For the sAOD comparison (Sect. 3.3), TMF backscatter profiles are converted to extinction with a lidar ratio of 50 sr, while for the backscatter-based analysis (Sect. 3.5) we retain the native backscatter units and perform a direct comparison with ATLID L1 β_{aer}.

https://doi.org/10.5194/egusphere-2026-4358
Preprint. Discussion started: 29 July 2026
© Author(s) 2026. CC BY 4.0 License.

2.4.2 Observatoire de Haute-Provence (OHP)

The Observatoire de Haute-Provence (OHP; 43.94° N, 5.71° E, 683 m a.s.l.), located in southern France and operated by LATMOS/IPSL within the NDACC network, has provided continuous stratospheric aerosol observations since the early 1990s using two independent lidar systems: LiO3S, operating at 355 nm, and LTA operating at 532 nm (Khaykin et al., 2017). In this study we use the LiO3S aerosol measurements at 355 nm, acquired at a mean rate of 10-12 nights per month (Godin-Beekmann et al., 2003; Khaykin et al., 2017). Vertical profiles of stratospheric aerosols are retrieved using the Sasano-Fernald inversion method, providing aerosol backscatter and extinction coefficients; the scattering ratio is computed as the ratio of total (molecular plus aerosol) to molecular backscatter, where the molecular contribution is derived from ECMWF meteorological analyses. The resulting profiles are reported at 150 m vertical resolution. A more detailed description of the instrument, retrieval methodology, and uncertainty budget is provided by Khaykin et al. (2017) and references therein.

OHP lidar data have previously been used for the validation of SAGE III/ISS aerosol extinction profiles (Knepp et al., 2020), demonstrating the suitability of this dataset as an independent stratospheric reference. In the present study, LiO3S backscatter profiles at 355 nm are treated identically to the TMF dataset and serve as an independent, ground-based validation reference at a Northern Hemisphere mid-latitude site in a different longitude sector. For the sAOD comparison (Sect. 3.3), the thermal tropopause altitude is obtained from the ECMWF meteorological data provided with the L2A product, and backscatter profiles are converted to extinction using a lidar ratio of 50 sr; for the backscatter-based analysis (Sect. 3.5), we retain the native backscatter units and perform a direct comparison with ATLID L1 β_{aer}.

2.5 Collocation methodology

ATLID and SAGE III/ISS profiles are collocated using the following criteria: a maximum spatial separation of 50 km, computed using the haversine formula between the SAGE III occultation tangent point and each individual ATLID footprint, and a maximum temporal difference of 12 h between the SAGE III occultation time and the ATLID overpass. For each SAGE III occultation satisfying these criteria, all ATLID Level-1 profiles falling within the collocation window are averaged together, and the resulting mean profile is interpolated onto the SAGE III vertical grid with 500 m step. The exact time difference between each collocated ATLID mean profile and the corresponding SAGE III occultation is recorded and displayed in the individual comparison figures.

For ground-based lidar collocations, the same temporal criterion of 12 h is applied, with the spatial criterion adapted to the fixed station geometry: all ATLID overpasses occurring within a great-circle distance of 100 km from each lidar station are considered.

2.6 Comparison metrics

The agreement between ATLID and reference instruments is quantified using the following metrics, computed for the full collocation dataset.

https://doi.org/10.5194/egusphere-2026-4358
Preprint. Discussion started: 29 July 2026
© Author(s) 2026. CC BY 4.0 License.

Table 1. Comparison metrics used in this study to evaluate ATLID L1 and L2 extinction products against SAGE III/ISS and ground-based lidar.

Metric	Definition and notes
Absolute bias	$\Delta\alpha(z) = \alpha_{\mathrm{ATLID}}(z) - \alpha_{\mathrm{ref}}(z)$, where α_{ref} is the SAGE III/ISS or ground-based lidar extinction.
Relative bias	$\delta\alpha(z) = \Delta\alpha(z)/\alpha_{\mathrm{ref}}(z) \times 100\,\%$. Median differences are reported to characterize the distributions.
Std deviation	$\sigma_{\Delta\alpha}(z)$: standard deviation of $\Delta\alpha$ across the collocation ensemble at each altitude level.
Extinction scatter	Point-to-point comparison using 2D density histograms. Evaluated via linear regression (slope) and Pearson R.
sAOD	Stratospheric AOD integrated from the ATLID tropopause $+1$ km to 30 km. Compared via a 1:1 scatter diagram with linear regression fits.
Relative sAOD bias	$(\mathrm{sAOD}_{\mathrm{ATLID}} - \mathrm{sAOD}_{\mathrm{ref}})/\mathrm{sAOD}_{\mathrm{ref}} \times 100\,\%$. Evaluated as a function of latitude and time.

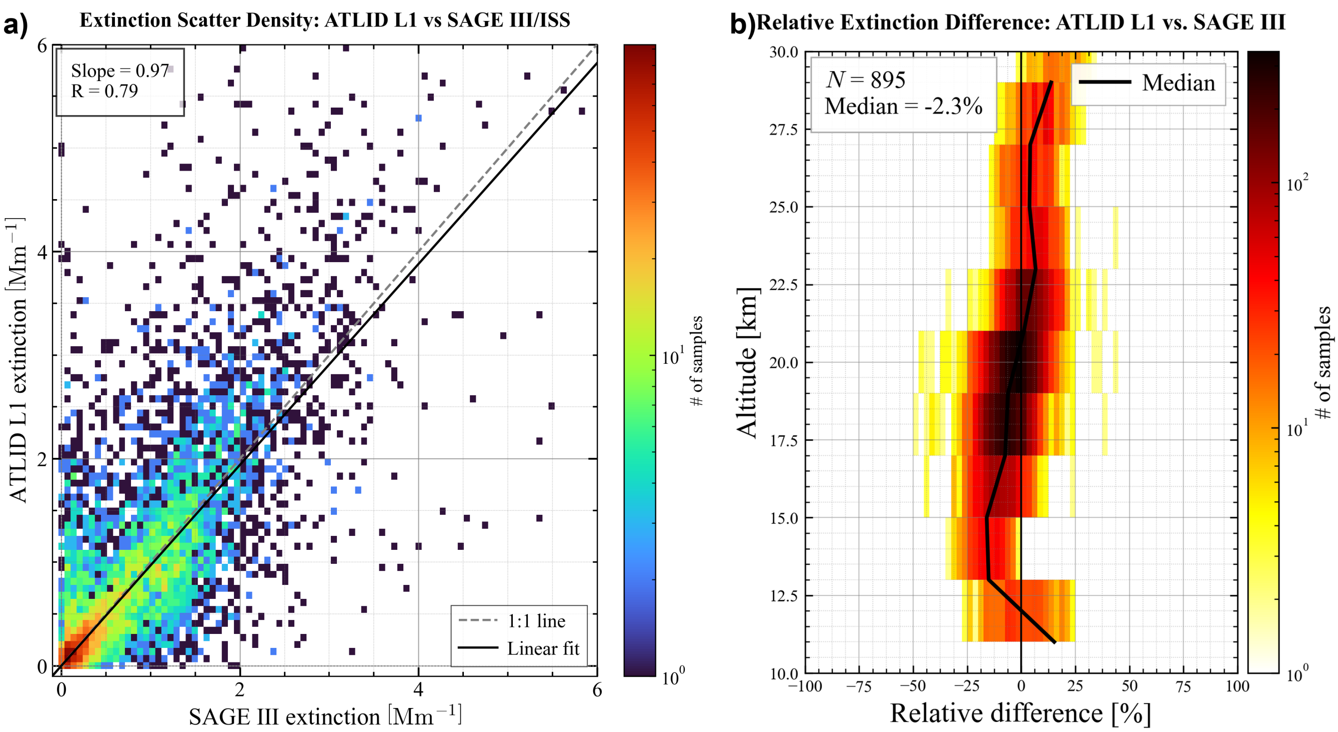

Figure 1. Comparison between ATLID L1 and SAGE III/ISS extinction coefficients. **a)** 2D density histogram for all collocated altitude-level pairs. The grey dashed line is the 1:1 reference; the solid black line is the ordinary least-squares linear regression (slope = 0.97, $R = 0.79$). **b)** Distribution of the relative difference as a function of altitude ($N = 895$ collocated profiles; see Sect. 2.5 for the definition of the collocation criteria). The solid black line shows the altitude-resolved median profile; the thin vertical line marks zero relative difference. The overall median is $-2.3\,\%$. For both panels, the colour scale gives the number of samples per bin on a logarithmic scale.

https://doi.org/10.5194/egusphere-2026-4358
Preprint. Discussion started: 29 July 2026
© Author(s) 2026. CC BY 4.0 License.

3 Results

The following subsections present the validation results in a logical sequence. We first establish the dataset characteristics (Sect. 3.1) and quantify the agreement between ATLID L1 and SAGE III/ISS at the profile level (Sect. 3.2) and in terms of integrated stratospheric AOD (Sect. 3.3). We then examine the spatio-temporal distribution of the relative sAOD bias (Sect. 3.4) and test the consistency of these findings against an independent, comparison with ground-based backscatter observations at OHP and TMF (Sect. 3.5). Finally, we place the L1 results in context by demonstrating the limitations of the native Level-2 product across all aerosol regimes (Sect. 3.6).

3.1 Overview of the collocation dataset

Over the study period from August 2024 to April 2026, the ATLID-SAGE III/ISS collocation procedure described in Sect. 2.5 produced a total of 895 co-located profile pairs, providing a statistically robust sample for the evaluation of ATLID performance across diverse atmospheric conditions. The number of co-located overpasses with the ground-based lidar stations is considerably smaller, reflecting the fixed-station geometry and the 25-day repeat cycle of EarthCARE: 55 events at TMF and 26 at OHP.

3.2 Altitude-resolved extinction comparison with SAGE III/ISS

The comparison between ATLID L1 and SAGE III/ISS extinction coefficients is presented in Fig. 1. Figure 1a displays all collocated altitude-level pairs as a 2D density histogram, in which the colour scale encodes the local sample count on a logarithmic scale. The bulk of the distribution is concentrated in the range 0-2 $\mathrm{Mm^{-1}}$, consistent with the dominance of near-background aerosol conditions in the dataset (Sect. 3.1). A linear regression through the full sample yields a slope of 0.97 and a correlation coefficient of $R = 0.79$, indicating a reasonably strong point-to-point correlation with a slight systematic underestimation of SAGE III/ISS extinction by ATLID L1 ($\sim$3 %). The scatter is substantial: a significant population of points lies well above the 1:1 line at low extinction (SAGE III/ISS $< 2\,\mathrm{Mm^{-1}}$), consistent with the additive retrieval noise floor.

Figure 1b presents the distribution of the relative difference $(\alpha_{\mathrm{L1}} - \alpha_{\mathrm{SAGE}})/\alpha_{\mathrm{SAGE}}$ as a function of altitude for the full set of $N = 895$ collocated profiles (see Sect. 2.5). The overall median relative difference is $-2.3\,\%$, confirming the near-zero systematic bias suggested by the regression slope in Fig. 1a and consistent with the near-unity sAOD regression reported in Sect. 3.3. The spread is large at all altitudes, with the distribution spanning approximately $\pm$25 % between the 10th and 90th percentiles, reflecting the dominant contribution of retrieval noise to individual altitude-level comparisons under background conditions.

The altitude profile of the median bias (solid black line in Fig. 1b) reveals a distinct vertical structure. In the lowermost stratosphere (approximately 10-13 km), the median is moderately positive ($\sim +10\,\%$), indicating that ATLID L1 slightly overestimates SAGE III/ISS extinction near the tropopause. Between approximately 13 and 17 km, the median transitions sharply toward negative values, reaching its most negative excursion of approximately $-15\,\%$ in the lower stratosphere. In the main aerosol layer (17-25 km), the median stabilises, indicating a consistent moderate underestimation by ATLID L1 throughout the

https://doi.org/10.5194/egusphere-2026-4358
Preprint. Discussion started: 29 July 2026
© Author(s) 2026. CC BY 4.0 License.

bulk of the Junge layer. Above 25 km, the median progressively approaches zero, consistent with both instruments approaching their respective noise floors as the aerosol signal weakens. The small overall median of $-2.3\,\%$ thus results from a partial cancellation between the positive near-tropopause contribution and the negative bias dominating the main aerosol layer; the underlying altitude-dependent structure, discussed further in Sect. 4.1, constitutes a more physically meaningful signature than the single-number summary statistic.

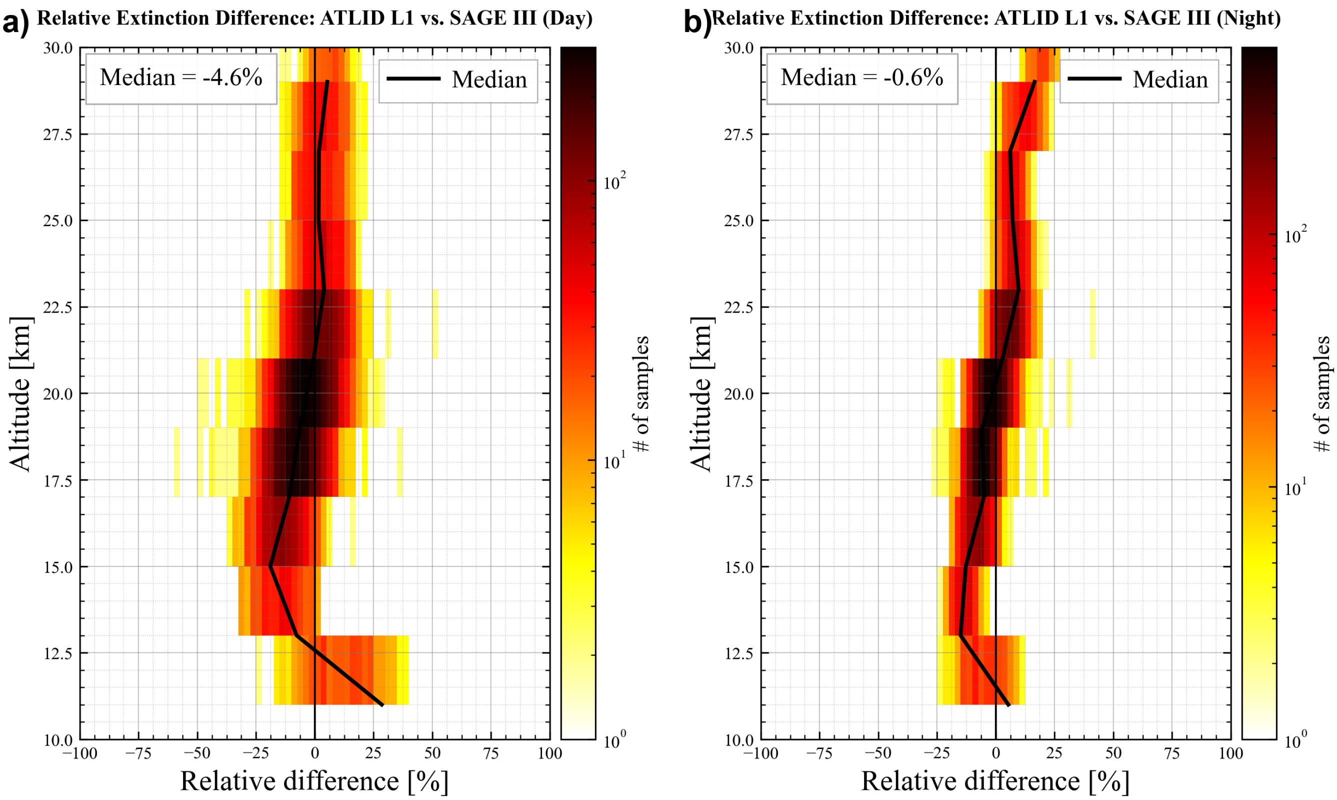

Figure 2. Relative extinction difference $(\alpha_{\mathrm{L1}} - \alpha_{\mathrm{SAGE}})/\alpha_{\mathrm{SAGE}}$ between ATLID L1 and SAGE III/ISS as a function of altitude, shown separately for **(a)** daytime and **(b)** nighttime SAGE III/ISS occultations. The colour scale gives the number of samples per bin on a logarithmic scale. The solid black line shows the altitude-resolved median; the inset in each panel reports the overall median relative difference over the 12-30 km range.

3.2.1 Day-night dependence of the altitude-resolved bias

To assess whether the altitude-dependent bias structure identified above is affected by solar illumination, we separated the collocation ensemble based on two independent daytime/nighttime criteria: the local solar time (LST) of the EarthCARE overpass, with $06{:}00 \leq \mathrm{LST} \leq 18{:}00$ classified as daytime and the remainder as nighttime; and the ATLID solar elevation angle (SEA) at the collocation point ($\mathrm{SEA} > 0°$ classified as daytime, $\mathrm{SEA} \leq 0°$ as nighttime). Both criteria gave consistent

https://doi.org/10.5194/egusphere-2026-4358
Preprint. Discussion started: 29 July 2026
© Author(s) 2026. CC BY 4.0 License.

classifications, and the relative difference profiles were recomputed for each subset (Fig. 2). Both panels show 2D histograms of the relative difference $(\alpha_{\mathrm{L1}} - \alpha_{\mathrm{SAGE}})/\alpha_{\mathrm{SAGE}}$ as a function of altitude.

The day and night subsets exhibit remarkably similar vertical structures. In both cases, the median bias is slightly positive in the lowermost stratosphere (around 12-13 km), turns negative in the lower to middle stratosphere, and gradually returns toward zero above approximately 25 km, closely mirroring the behaviour of the combined ensemble in Fig. 1b. The main aerosol layer (17-25 km) is again characterised by a moderate negative bias of order -5 to $-10\,\%$ for both day and night conditions, while the spread of the distribution remains large for the daytime subset at all altitudes, consistent with the dominant contribution of retrieval noise under near-background aerosol loading.

Quantitatively, the vertically integrated median bias differs only slightly between the two subsets, with values of $-4.6\,\%$ for day and $-0.6\,\%$ for night. However, a more striking difference between the two subsets concerns the *spread* of the distribution: the nighttime collocations exhibit a substantially narrower dispersion at all altitudes compared to daytime, as is clearly visible in Fig. 2. This is consistent with the well-known increase in SAGE III/ISS measurement noise during daytime occultations, which are affected by solar background radiation on the detector. Quantitatively, the mean standard deviation of the relative differences, averaged over all altitude bins in the 12-30 km range, amounts to $\sim$ 32% for the daytime subset and $\sim$ 17% for the nighttime subset, confirming the improved signal-to-noise performance of nighttime occultations.

https://doi.org/10.5194/egusphere-2026-4358
Preprint. Discussion started: 29 July 2026
© Author(s) 2026. CC BY 4.0 License.

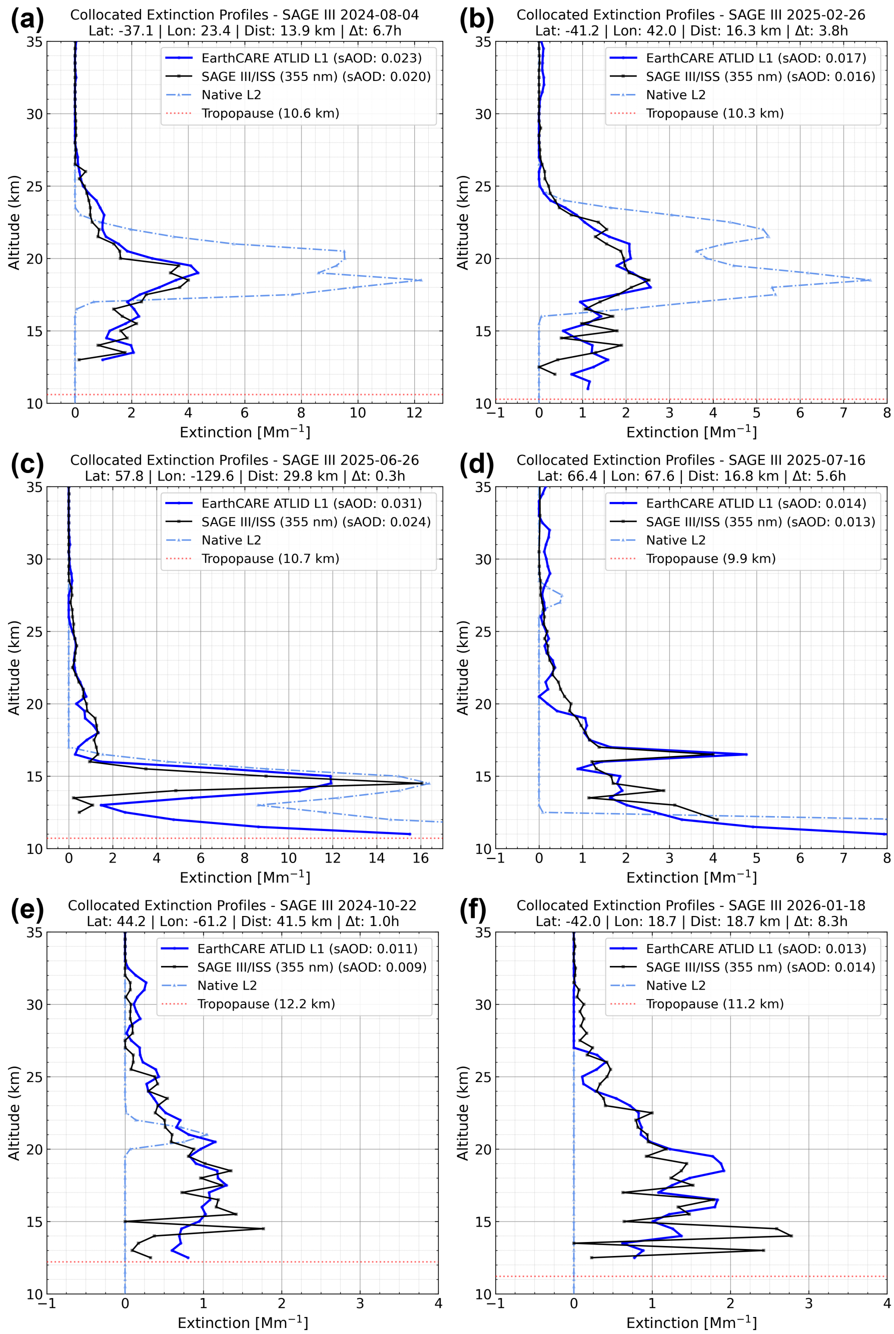

Figure 3. Collocated extinction profiles from SAGE III/ISS, ATLID L1, and native ATLID L2 for selected case studies. **(a, b)** Southern Hemisphere Ruang volcanic plume (older layer in b): L1 and SAGE III/ISS show coherent vertical structure, while L2 overestimates the peak. **(c, d)** Boreal wildfire smoke: in the strong layer (c), residual L1/SAGE differences likely reflect plume spatial heterogeneity, and L2 again overestimates the peak; in the weaker layer (d), L2 misses the layer entirely. **(e, f)** Background conditions ($< 2\,\mathrm{Mm}^{-1}$): L2 erroneously reports a narrow peak in place of a diffuse layer in (e), and returns zero extinction throughout in (f).

https://doi.org/10.5194/egusphere-2026-4358
Preprint. Discussion started: 29 July 2026
© Author(s) 2026. CC BY 4.0 License.

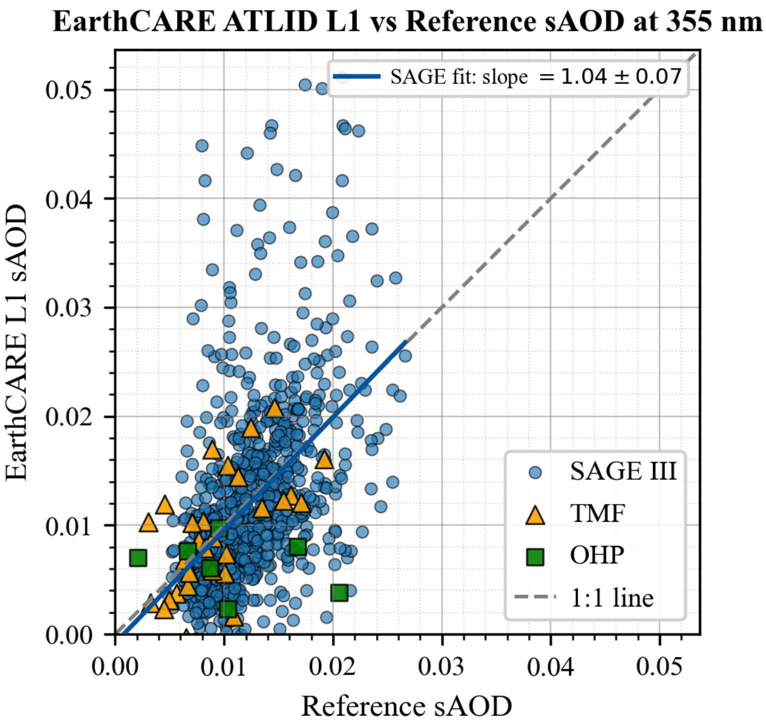

Figure 4. Scatter diagram of ATLID L1 sAOD versus reference sAOD from SAGE III/ISS (circles), TMF (triangles), and OHP (squares), integrated from the ATLID-derived tropopause +1 km to 30 km. The dashed grey line is the 1:1 reference. The solid blue line shows the linear regression fit to the SAGE III/ISS matchups: slope = 1.04 ± 0.07 (±1 standard error), intercept = $(-0.8 \pm 0.9) \times 10^{-3}$, $R = 0.67$.

The small day-night offset in median bias is well within the altitude-to-altitude variability of the median profiles and considerably smaller than the typical percentile spread at a given height, indicating that the ATLID L1 vs SAGE III/ISS extinction bias is, to first order, insensitive to the solar illumination conditions at the time of the ATLID overpass. We therefore attribute the modest day-night differences primarily to changes in the signal-to-noise characteristics of the SAGE III/ISS solar occultation measurements themselves rather than to any systematic dependence of the ATLID L1 retrieval on illumination conditions.

3.2.2 Representative profile case studies

Figure 3 presents six representative collocation case studies selected to illustrate the three distinct stratospheric aerosol regimes sampled in this study: volcanic plumes, wildfire smoke, and low aerosol background conditions. In each panel, the ATLID L1 profile (solid blue line) and the native ATLID L2 retrieval (dashed light blue line) are compared against the SAGE III/ISS reference (solid black line); the local tropopause altitude is indicated by a horizontal pink dashed line. Comparing these diverse scenes highlights the contrasting behaviour of the ATLID L1 and native L2 extinction products under varying aerosol loadings.

https://doi.org/10.5194/egusphere-2026-4358
Preprint. Discussion started: 29 July 2026
© Author(s) 2026. CC BY 4.0 License.

Panels (a) and (b) correspond to Southern Hemisphere collocations affected by the Ruang volcanic plume, acquired on 4 August 2024 (lat $-37.1°$, $\Delta t = 6.7$ h) and 26 February 2025 (lat $-41.2°$, $\Delta t = 3.8$ h), respectively. In both cases, ATLID L1 and SAGE III/ISS reproduce a coherent vertical structure with a pronounced extinction peak in the 14-18 km range, consistent with the known altitude of the volcanic injection layer after its poleward transport (K26). The native L2 product systematically overestimates the peak extinction in both panels, yielding values up to a factor of ~2-3 above the SAGE III/ISS reference.

Panels (c) and (d) show collocations within boreal wildfire smoke layers, acquired on 26 June 2025 (lat $57.8°$, $\Delta t = 0.3$ h) and 16 July 2025 (lat $66.4°$, $\Delta t = 5.6$ h), respectively. The stronger layer in panel (c) (ATLID L1 sAOD $= 0.031$) is well captured by both ATLID L1 and SAGE III/ISS, with a sharp extinction peak near 12-14 km reaching approximately 8-16 Mm^{-1}; residual differences between L1 and SAGE III/ISS at the peak are likely attributable to the spatial heterogeneity of the smoke plume given the ~30 km collocation distance, rather than to a systematic retrieval error. The L2 product again overestimates the peak extinction in panel (c). In the weaker companion layer of panel (d) (SAGE III/ISS sAOD $= 0.013$), ATLID L1 and SAGE III/ISS remain in reasonable agreement across the stratospheric column, while the native L2 product fails to detect the layer entirely, returning near-zero extinction throughout the profile.

Panels (e) and (f) represent background conditions with stratospheric aerosol optical depths below approximately 0.015, acquired on 22 October 2024 (lat $44.2°$, $\Delta t = 1.0$ h) and 18 January 2026 (lat $-42.0°$, $\Delta t = 8.3$ h), respectively. Under these low-loading conditions, ATLID L1 and SAGE III/ISS consistently show a diffuse, weakly structured extinction profile with values below ~2 Mm^{-1} throughout the stratospheric column. The L2 retrieval fails in qualitatively different ways in each case: in panel (e), it produces a spurious, narrow extinction peak near 13 km with no counterpart in either the L1 or SAGE III/ISS profiles; in panel (f), it returns strictly zero extinction across the entire stratospheric column, representing a complete retrieval failure. Together, these six case studies demonstrate that the skill of the native ATLID L2 stratospheric aerosol retrieval degrades markedly with decreasing aerosol loading, while the L1-based K26 product maintains consistent agreement with SAGE III/ISS across all regimes, providing a clear rationale for its use as the primary extinction estimate throughout the remainder of this study.

3.3 Stratospheric AOD comparison

Figure 4 presents the scatter diagram of ATLID L1 sAOD against the reference sAOD from SAGE III/ISS and the available ground-based lidar stations (TMF, OHP), integrated from the ATLID tropopause $+1$ km to 30 km. Reference sAOD values span approximately 0-0.030 for the SAGE III/ISS matchups, covering background conditions, the volcanic perturbation associated with the Ruang eruption (April-May 2024), and the wildfire smoke events of boreal summer 2025.

A linear regression applied to the SAGE III/ISS matchups yields a slope of 1.04 ± 0.07, an intercept of $(-0.8 \pm 0.9) \times 10^{-3}$ $(R = 0.67)$, indicating that the ATLID L1 product is, on average, essentially unbiased with respect to SAGE III/ISS integrated sAOD. However, the scatter around the regression line is not uniform across the dynamic range and reveals contrasting behaviour between the low- and high-aerosol-loading regimes. While the dense core of the data remains broadly consistent with the 1:1 line, the high-loading regime (reference sAOD > 0.010) exhibits an asymmetric dispersion. Specifically, there is a

https://doi.org/10.5194/egusphere-2026-4358
Preprint. Discussion started: 29 July 2026
© Author(s) 2026. CC BY 4.0 License.

prominent subset of ATLID L1 retrievals that yield significantly higher values than the SAGE III/ISS reference, creating a pronounced positive tail in the distribution.

Among the ground-based reference instruments, the TMF matchups (orange triangles) scatter on both sides of the 1:1 line without a clear directional offset, broadly mirroring the noise-dominated behaviour of the SAGE III/ISS ensemble at comparable sAOD levels. The OHP matchups (green squares) follow the same qualitative low-/ high-loading pattern, with a tendency for points to fall below the 1:1 line as the reference sAOD increases; more matchups lie below than above the regression line overall, foreshadowing the systematic negative offset identified independently for this station from the point-to-point backscatter comparison in Sect. 3.5.

3.4 Latitudinal and temporal distribution of the relative sAOD bias

Figure 5 presents the relative sAOD difference $(\mathrm{sAOD_{L1}} - \mathrm{sAOD_{ref}})/\mathrm{sAOD_{ref}}$ as a function of latitude (panel a) and time (panel b) for the SAGE III/ISS, TMF, and OHP matchups. Across all matchups, the relative sAOD bias has a global mean of $-3.2\,\%$ with a standard deviation of $65.7\,\%$, indicating a near-zero systematic offset combined with a large point-to-point scatter.

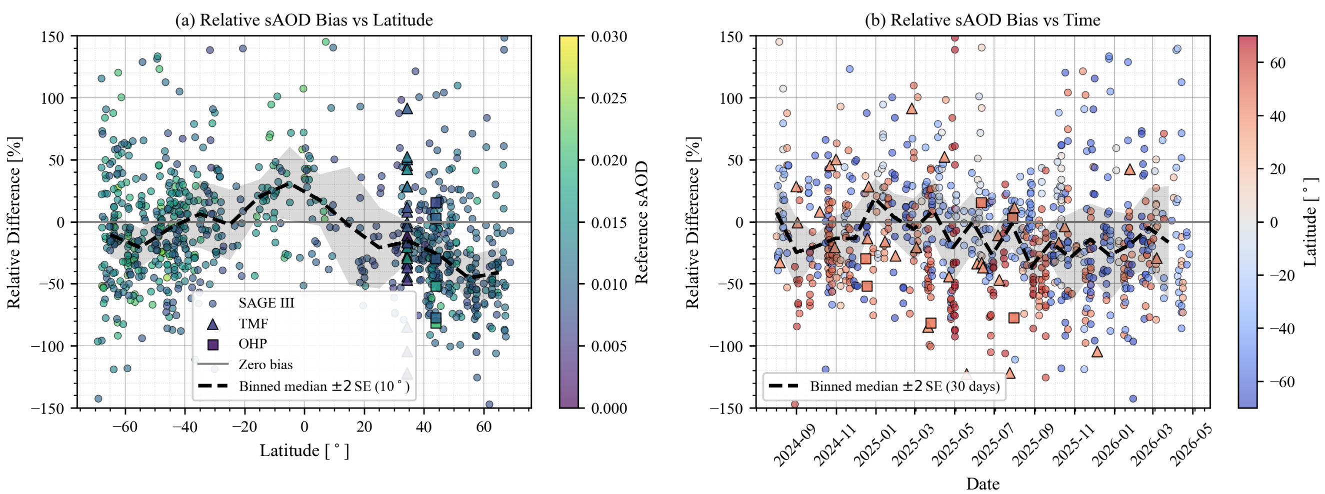

Figure 5. Relative sAOD bias of ATLID L1 with respect to SAGE III/ISS (circles), TMF (triangles), and OHP (squares) as a function of (a) latitude and (b) time. Symbol colours encode the reference sAOD in panel (a) and the collocation latitude in panel (b). The solid grey line marks zero bias; the dashed black line is the binned median relative difference (10° latitude bins in panel a, 30-day windows in panel b), and the surrounding grey shaded envelope shows its ±2 standard-error (±2 SE) interval, i.e. an approximate 95 % confidence range on the median in each bin.

The latitudinal distribution (Fig. 5a) reveals a clear meridional gradient in the SAGE III/ISS-based comparisons, with ATLID L1 exhibiting a systematic negative bias in the Northern Hemisphere extratropics that increases with latitude. The grey shaded envelope around the dashed line represents the ±2 standard-error (±2 SE) interval of the binned median, i.e. an

https://doi.org/10.5194/egusphere-2026-4358
Preprint. Discussion started: 29 July 2026
© Author(s) 2026. CC BY 4.0 License.

approximate 95 % confidence range in each bin; it is narrow where collocations are dense (the tropics and NH mid-latitudes) and broad in the sparsely sampled polar bins, providing a visual guide to which median excursions are statistically robust rather than an artefact of limited sampling. The scatter is large at all latitudes, with individual relative differences frequently exceeding ±50 %, consistent with the standard deviation reported above. Among the ground-based stations, the TMF matchups (triangles, 34° N) span a wide range of both positive and negative relative biases, while the OHP matchups (squares, 44° N), though limited in number, are predominantly negative, consistent with the tendency noted in Sect. 3.3 and confirmed independently in Sect. 3.5.

The temporal distribution (Fig. 5b) shows no obvious secular drift over the 20-month record, indicating broad stability of the ATLID L1 calibration throughout the study period. The apparent see-saw pattern of the 30-day binned median likely reflects the changing latitudinal sampling of SAGE III/ISS, with intervals dominated by Northern Hemisphere extratropical matchups showing a more negative bias, consistent with the low bias identified for NH mid- to high-latitude comparisons in Fig. 5a, rather than any systematic temporal drift of the ATLID L1 product. The ±2 SE envelope on the median widens during intervals with fewer collocations, and no monotonic trend emerges beyond this envelope, reinforcing the absence of a significant temporal drift and the broad stability of the ATLID L1 calibration.

https://doi.org/10.5194/egusphere-2026-4358
Preprint. Discussion started: 29 July 2026
© Author(s) 2026. CC BY 4.0 License.

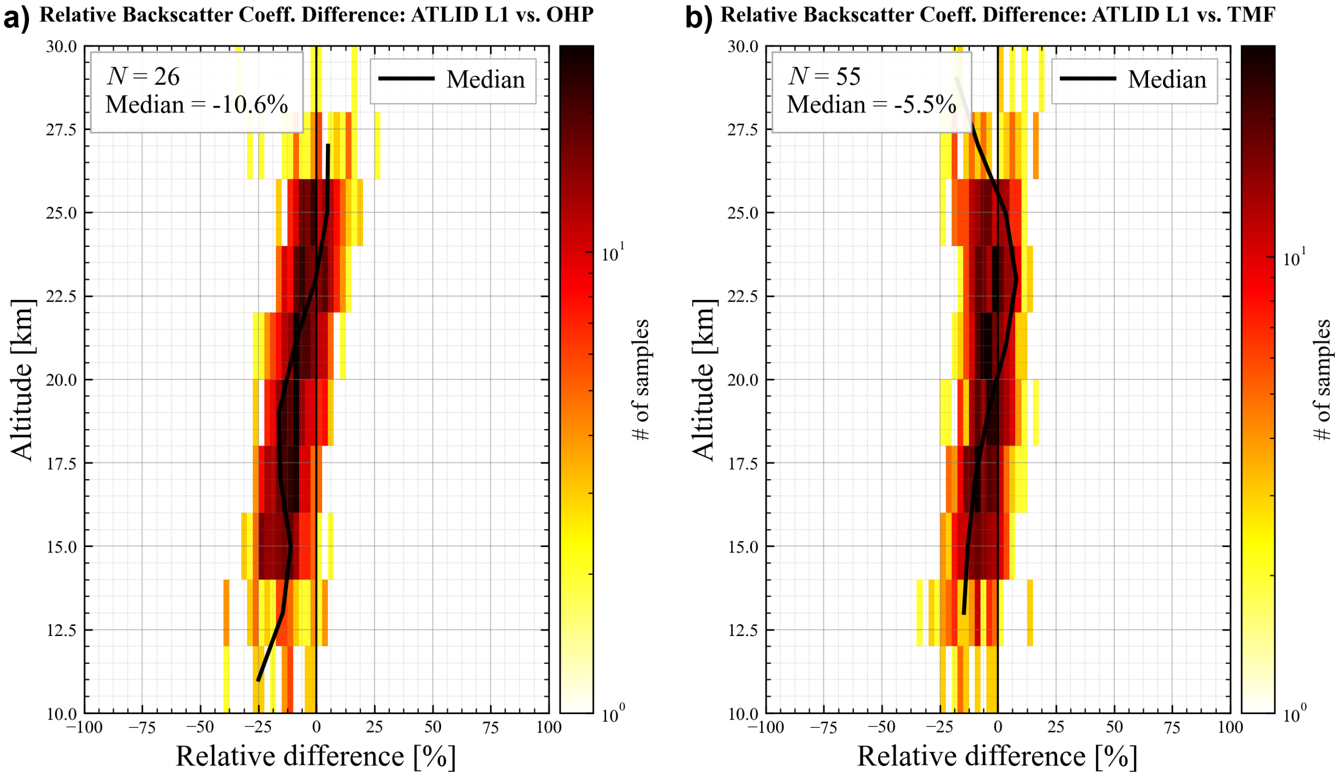

Figure 6. Distribution of the relative difference between ATLID L1 and ground-based lidar particulate backscatter coefficients as a function of altitude for **(a)** OHP ($N = 26$ collocated overpasses) and **(b)** TMF ($N = 55$ collocated overpasses). In each panel, the colour scale gives the number of samples per bin on a logarithmic scale. The solid black line shows the altitude-resolved median profile; the thin vertical line marks zero relative difference. The overall median relative differences are $-10.6\,\%$ (OHP) and $-5.5\,\%$ (TMF).

3.5 Point-to-point backscatter coefficient comparison: OHP and TMF

The comparisons presented above rely, to varying degrees, on the conversion from ATLID L1 backscatter to extinction via a lidar ratio (Eq. (1)). This lidar ratio is taken from the ATLID L2 product when available, and set to a fixed value of 50 sr otherwise (see Sect. 2.2). To isolate the contribution of this conversion step from that of the underlying scattering-ratio retrieval, we additionally compare ATLID L1 particulate backscatter coefficients directly against collocated ground-based lidar backscatter profiles at OHP and TMF, applying the same point-to-point relative-difference metric defined in Sect. 2.6 but evaluated on β_{aer} rather than on extinction.

Figure 6 shows the resulting distributions of the relative backscatter difference as a function of altitude for the $N = 26$ OHP overpasses (panel a) and the $N = 55$ TMF overpasses (panel b). At OHP, the overall median relative difference is $-10.6\,\%$, while at TMF it amounts to $-5.5\,\%$. Both values are negative, confirming a systematic tendency for ATLID L1 to underestimate ground-based backscatter, consistent with the underestimation identified in the SAGE III/ISS extinction comparison (Sect. 3.2). The difference in magnitude between the two stations (OHP exhibiting a roughly twice as large negative offset as TMF) may

https://doi.org/10.5194/egusphere-2026-4358
Preprint. Discussion started: 29 July 2026
© Author(s) 2026. CC BY 4.0 License.

293 reflect the smaller OHP sample size, differences in the altitude ranges effectively sampled by each lidar, or a genuine site-
294 dependent component.

295 Interestingly, both lidar stations confirm a slight negative bias in the lower stratosphere, consistent with the behaviour found
296 in the SAGE III/ISS comparison. The scatter of the differences is also similar to that observed for the nighttime SAGE III/ISS
297 collocations, as all lidar collocations are nighttime observations. The OHP profile displays a similar structure, with the negative
298 bias concentrated between 11 and 23 km and a clearer positive excursion near 23-27 km. Because both comparisons are, by
299 construction, independent of the lidar ratio, this three-instrument consistency strongly indicates that the altitude-dependent bias
300 structure identified throughout Sect. 3.2 originates predominantly in the Level-1 scattering-ratio retrieval itself, rather than in
301 the extinction-conversion step (Sect. 2.2).

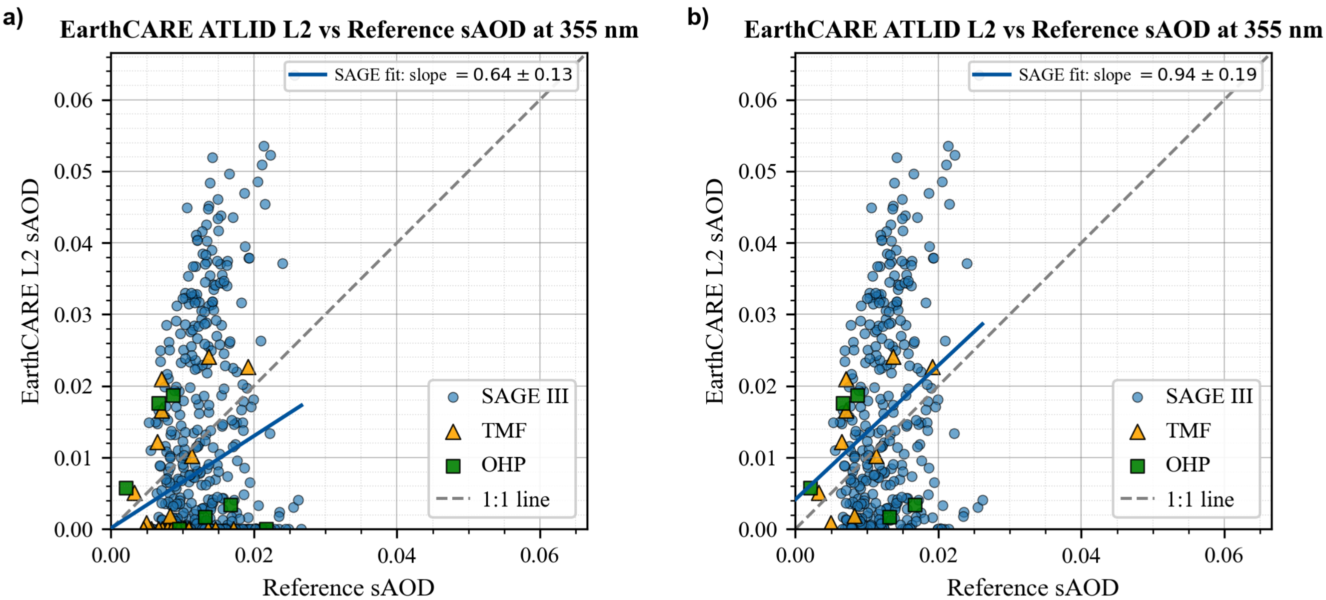

Figure 7. Scatter diagrams of native ATLID L2 sAOD versus reference sAOD from SAGE III/ISS (circles), TMF (triangles), and OHP (squares), integrated from the ATLID-derived tropopause +1 km to 30 km. **(a)** All collocated matchups, including cases for which the L2 processor returns no stratospheric retrieval ($\mathrm{sAOD_{L2}} = 0$, visible along the horizontal axis). The linear regression fit to the SAGE III/ISS matchups ($N = 652$) yields a slope of 0.64 ± 0.13 and an intercept of $(0.1 \pm 1.7) \times 10^{-3}$ ($R = 0.19$). **(b)** Same comparison but restricted to actual retrievals ($\mathrm{sAOD_{L2}} > 0$); the null retrievals ($\mathrm{sAOD_{L2}} = 0$) shown along the horizontal axis in panel (a) are here excluded from both the display and the fit. The regression to the SAGE III/ISS matchups ($N = 331$) then yields a slope of 0.94 ± 0.19 with a positive intercept of $(4.1 \pm 2.6) \times 10^{-3}$ ($R = 0.26$). In both panels, the dashed grey line is the 1:1 reference and quoted uncertainties are one standard error.

302 ### 3.6 Rationale for the Level-1-based retrieval: comparison with native Level-2 products

303 Having established the robustness of the Level-1-based (K26) extinction product across diverse stratospheric conditions, we
304 now evaluate the added value of this approach relative to the native ATLID Level-2 (L2) aerosol retrieval. Figure 7a shows the

https://doi.org/10.5194/egusphere-2026-4358
Preprint. Discussion started: 29 July 2026
© Author(s) 2026. CC BY 4.0 License.

scatter of L2 stratospheric AOD against the reference sAOD from SAGE III/ISS, TMF, and OHP. A linear regression to the SAGE III/ISS matchups yields a slope of only 0.64 and an intercept of 0.1×10^{-3}, well below the near-unity slope obtained for the L1 product over the same matchup ensemble (slope $= 1.04 \pm 0.07$, intercept $= (-0.8 \pm 0.9) \times 10^{-3}$; Sect. 3.3, Fig. 4). The L2 product is also visibly sparser than the L1 product in Fig. 7a, reflecting the frequent occurrence of fill values noted in Sect. 2.2.

Restricting the comparison to profiles for which the L2 processor returns an actual stratospheric retrieval ($\mathrm{sAOD_{L2}} > 0$; Fig. 7b) partially compensates for the systematic underestimation seen in panel (a): the SAGE III/ISS regression slope rises from 0.64 ± 0.13 to 0.94 ± 0.19, formally consistent with unity. This improvement is, however, largely artificial. It results from the removal of the numerous null retrievals ($\mathrm{sAOD_{L2}} = 0$) that pull the full-sample slope downward, rather than from any genuine skill of the L2 product. Indeed, the correlation remains very weak ($R = 0.26$) and the fit acquires a significantly positive intercept of $(4.1 \pm 2.6) \times 10^{-3}$, indicating that the retained L2 retrievals scatter almost independently of the true aerosol loading and, on average, overestimate the low-sAOD background. Even when the L2 processor does converge to a non-zero solution, the resulting sAOD is therefore only loosely tied to the reference value, and the apparent near-unity slope in panel (b) should not be interpreted as evidence of reliable quantitative agreement.

At low reference sAOD ($\lesssim 0.02$), where the bulk of the dataset lies, L2 retrievals show essentially no relationship with the reference values: some matchups return spuriously high sAOD (up to 0.05-0.06) while others return values close to zero, regardless of the true aerosol loading. This behaviour is illustrated at the profile level by the selected case studies shown in Fig. 3, spanning the three aerosol regimes sampled in this study. Taken together, the aggregate sAOD comparison and the case-level profiles demonstrate that the skill of the native L2 retrieval degrades sharply as the aerosol loading decreases, and justify the systematic use of the L1-based K26 product as the primary ATLID extinction estimate throughout the remainder of this study.

4 Discussion

We now discuss the possible physical origins of the bias patterns identified in Sect. 3, the practical implications of the L1/L2 contrast for ATLID data users, and the main limitations of the present analysis.

4.1 Altitude/Latitude-dependent structure of the ATLID bias

The altitude-dependent bias identified independently in the SAGE III/ISS extinction comparison (Sect. 3.2) and in the OHP and TMF backscatter comparisons (Sect. 3.5) is mainly consistent across the three instruments: all three agree in the lower-to-mid stratosphere, whereas near the tropopause the sign of the bias differs between SAGE III/ISS and the ground-based lidars, with a positive bias for SAGE III/ISS. These features point toward a small number of plausible physical origins.

The positive offset near the tropopause is specific to the SAGE III/ISS comparison: OHP and TMF both remain negative at the same altitudes rather than showing a comparable positive excursion (Sect. 3.5), which argues against a reference-independent artefact such as genuine cloud contamination of the ATLID profiles and instead points to a SAGE-specific factor, for instance,

https://doi.org/10.5194/egusphere-2026-4358
Preprint. Discussion started: 29 July 2026
© Author(s) 2026. CC BY 4.0 License.

differences in effective tropopause altitude or the explicit SAGE III/ISS screening of aerosol-cloud mixtures near the tropopause (Sect. 2.3). The pronounced negative excursion through the lower-to-mid stratosphere, by contrast, is common to SAGE III/ISS, OHP, and TMF alike; while this consistency argues against the conversion step being the dominant driver and instead points to an origin within the Level-1 scattering-ratio retrieval itself, the exact physical mechanisms driving this distinct vertical bias structure require further investigation. Above ∼25 km, the convergence of both comparisons toward near-zero bias is most plausibly explained by both instruments approaching their respective noise floors as the aerosol signal weakens.

This behaviour is broadly consistent with the lessons learned from the CALIOP stratospheric aerosol product. Kar et al. (2019) showed that the improved Version 4 calibration of CALIOP enabled a reliable retrieval of stratospheric aerosol extinction, but also that agreement with SAGE III/ISS remains strongly latitude- and altitude-dependent: comparatively good in the tropical stratosphere between about 20 and 30 km, and substantially poorer at higher latitudes and near the tropopause, where differences can exceed 100 %. Those results are particularly relevant here because they show that, even for a mature elastic lidar product, the stratospheric regime remains challenging when the aerosol loading is weak and the signal-to-noise ratio is low.

ATLID itself exhibits an analogous latitudinal signature: the sAOD bias distribution (Sect. 3.4, Fig. 5a) shows a systematic negative bias in the Northern Hemisphere extratropics that increases with latitude. Part of this gradient may be linked to aerosol type rather than to latitude *per se*: the boreal wildfire smoke events sampled during this study are concentrated at Northern Hemisphere mid-to-high latitudes, and smoke particles are expected to depart more strongly from the fixed 50 sr lidar ratio used in the absence of a valid L2 value (Sect. 2.2) than aged background sulfate aerosol.

To further contextualize the degree of agreement observed between ATLID L1 and SAGE III/ISS, it is instructive to compare our results with other satellite intercomparison studies. For instance, Kovilakam et al. (2023) evaluated the consistency between SAGE III/ISS extinction and CALIOP backscatter-derived extinction (see their Fig. 13). They demonstrated that direct comparisons using a constant lidar ratio for CALIOP yielded regional biases frequently exceeding 50 % in the lower stratosphere and at higher latitudes. It was only after applying an empirical, altitude- and latitude-dependent scale factor to the CALIOP data that the differences relative to SAGE III/ISS were reduced to within ±20 %. In this context, the agreement found in our study without relying on any empirical post-scaling highlights the robust performance of the ATLID L1-based retrieval and the distinct advantage of its HSRL measurement capabilities in the stratosphere.

4.2 Implications of the Level-1/Level-2 contrast for data users

The clear contrast between the regression slopes obtained for the L1 (1.04) and native L2 (0.64) sAOD products against SAGE III/ISS (Sect. 3.6) has direct practical implications. The native L2 stratospheric aerosol product, in its current processing baseline, should not be relied upon for quantitative assessments of background or weakly perturbed stratospheric aerosol, the regime that dominates the EarthCARE record outside of the Ruang eruption and the 2025 boreal wildfire season, since it exhibits essentially no skill in this regime and frequently defaults to either spuriously elevated or null retrievals. The L1-based K26 product evaluated throughout this study provides a substantially more faithful representation of the true aerosol

https://doi.org/10.5194/egusphere-2026-4358
Preprint. Discussion started: 29 July 2026
© Author(s) 2026. CC BY 4.0 License.

loading across the full dynamic range sampled here, and we recommend its use, at least in the interim, for stratospheric aerosol monitoring and trend studies based on ATLID, pending future refinement of the operational L2 algorithm.

The quality of the SAGE III/ISS reference data is also important in interpreting these comparisons. The extinction profiles used here are derived from the 384 nm channel and converted to 355 nm using the 384-521 nm Ångström exponent, with profiles affected by transmission anomalies, cloud contamination, or large fractional uncertainty excluded following established quality-control recommendations (Knepp et al., 2020). SAGE III/ISS is therefore a robust and well-characterized reference, but not a noise-free one; some of the residual scatter in the ATLID comparison likely reflects the combined uncertainties of both instruments.

Beyond the reference dataset itself, the extinction retrieval relies on a lidar ratio that is either taken from the ATLID L2 product or, when unavailable, fixed at 50 sr regardless of aerosol type (Sect. 2.2). Although assuming a fixed lidar ratio is a theoretical source of uncertainty, it is unlikely to introduce a significant systematic bias in our dataset. For optically thick, fresh plumes (such as dense volcanic ash or absorbing wildfire smoke), the ATLID L2 processor generally provides reliable, directly measured lidar ratios that supersede the fallback. Conversely, for aged plumes and near-background stratospheric conditions where the L2 retrieval defaults to fill values, the true physical lidar ratio is expected to be close to the 50 sr assumed value. A full quantitative sensitivity analysis is left for future work, including a targeted test of the smoke-related, high-latitude hypothesis raised in Sect. 4.1. We note, however, that the qualitative consistency between the lidar-ratio-dependent SAGE III/ISS extinction comparison and the lidar-ratio-independent OHP backscatter comparison (Sect. 3.5) suggests that the dominant altitude-dependent bias pattern identified in this study is not primarily a lidar-ratio artefact.

5 Conclusions

We have presented a systematic validation of the ATLID stratospheric aerosol retrieval using 895 collocated SAGE III/ISS extinction profiles and ground-based backscatter measurements from OHP and TMF, covering the period August 2024-April 2026 and spanning background, volcanic, and wildfire aerosol conditions.

The Level-1-based (K26) extinction product, derived from the ATLID scattering ratio via a Level-2 lidar ratio, shows near-zero overall bias with respect to SAGE III/ISS, with a linear regression slope of 1.04 and an overall median relative extinction difference of $-2.3\,\%$ across all altitudes. At the integrated column level, ATLID L1 sAOD is essentially unbiased with respect to the reference, with a global mean relative sAOD bias of $-3.2\,\%$ across all matchups; the associated standard deviation of $65.7\,\%$, however, reflects a large point-to-point scatter dominated by retrieval noise under near-background aerosol loading. However, the altitude-resolved comparison reveals a consistent vertical structure: a pronounced underestimation in the lower-to-mid stratosphere (up to $-15\,\%$), and convergence toward zero above ~25 km. This altitude-dependent bias pattern is independently reproduced by the backscatter comparisons against OHP ($-10.6\,\%$ overall median) and TMF ($-5.5\,\%$ overall median), strongly suggesting it is an intrinsic feature of the ATLID L1 scattering-ratio retrieval rather than an artefact of the lidar-ratio conversion.

https://doi.org/10.5194/egusphere-2026-4358
Preprint. Discussion started: 29 July 2026
© Author(s) 2026. CC BY 4.0 License.

A further noteworthy result is the better nighttime performance of ATLID L1. The daytime collocations are visibly noisier, with a relative-difference standard deviation nearly twice as large as at night (∼32 % versus ∼17 %, averaged over the 12-30 km range); yet the global median bias remains close to zero in both cases, indicating that the retrieval is still accurate in a climatological sense. This behaviour is consistent with the HSRL capability of ATLID, which enables a much better daytime performance than a conventional elastic lidar such as CALIOP, despite the larger daytime background and associated retrieval noise (Feofilov et al., 2023).

In contrast, the native ATLID Level-2 stratospheric aerosol product exhibits severe limitations across most of the dynamic range sampled in this study. Against SAGE III/ISS, the full L2 sAOD ensemble yields a regression slope of only 0.64, an artificial negative bias driven by the frequent occurrence of null retrievals (fill values) under low-aerosol conditions. While restricting the analysis to successful L2 retrievals artificially raises the slope to near unity, the correlation remains very weak ($R = 0.26$) because the algorithm tends to overestimate the low-sAOD background and produces spurious narrow peaks. Furthermore, the L2 product systematically overestimates peak extinction in dense volcanic and wildfire plumes. Consequently, the L1-based K26 approach introduced in Khaykin et al. (2026) provides a substantially more faithful representation of stratospheric aerosol loading across all regimes and is recommended for ATLID-based stratospheric aerosol monitoring pending future refinements of the operational L2 algorithm.

The study demonstrates that EarthCARE ATLID is capable of consistently resolving stratospheric aerosol extinction across a wide range of conditions with an accuracy of a few percent on the mean extinction profile, making it a valuable addition to the existing observing system for stratospheric aerosol. Future work should extend the validation record, incorporate additional ground-based stations at a broader range of latitudes, and undertake a dedicated lidar-ratio sensitivity study to further constrain the residual altitude-dependent bias identified here.

Code availability. The ATLID L1B data processing code is available at https://doi.org/10.5281/zenodo.18155346 (Kadygrov and Khaykin, 2026). The collocation and statistical analysis code used to produce the results and figures presented in this paper is available at https://doi.org/10.5281/zenodo.21282209 (Poncet, 2026).

Data availability. EarthCARE ATLID data are available at https://earth.esa.int/eogateway/catalog/earthcare-l1-products (last access: 5 June 2026); SAGE III data are available at https://asdc.larc.nasa.gov/project/SAGE_III-ISS/g3bssp_6 (last access: 5 June 2026); NDACC lidar data are available at https://ndacc.larc.nasa.gov (last access: 5 January 2026).

Author contributions. SK conceived the study, EP performed the analysis and wrote the manuscript, TL provided TMF lidar data. SK and SGB provided OHP lidar data. All authors contributed to the final manuscript.

https://doi.org/10.5194/egusphere-2026-4358
Preprint. Discussion started: 29 July 2026
© Author(s) 2026. CC BY 4.0 License.

Competing interests. The contact author has declared that none of the authors has any competing interests.

Special issue statement. This article is part of the special issue "Early results from EarthCARE (AMT/ACP/GMD inter-journal SI)". It is not associated with a conference.

Acknowledgements. We thank the personnel of lidar stations (OHP and TMF) for conducting lidar measurements. The French lidar stations operate under support of French Institut National des Sciences de l'Univers (INSU) of the Centre National de la Recherche Scientifique (CNRS) and of Centre National d'Études Spatiales (CNES). Part of this research was carried out at the Jet Propulsion Laboratory, California Institute of Technology, under a contract with the National Aeronautics and Space Administration (80NM0018D0004), (NASA).

Financial support. This research has been supported by the Agence Nationale de la Recherche (grant no. PyroStrat 21-CE01-335 0007-01), and the Centre National d'Études Spatiales (grant no. EARTHCARE).

https://doi.org/10.5194/egusphere-2026-4358
Preprint. Discussion started: 29 July 2026
© Author(s) 2026. CC BY 4.0 License.

References

Baars, H., *et al.*: Validation of EarthCARE/ATLID aerosol profiling products with ground-based PollyNET lidars – case studies, *Atmos. Meas. Tech.*, 19, 3831–XXXX, https://doi.org/10.5194/amt-19-3831-2026, 2026.

Cisewski, M., Zawodny, J., Gasbarre, J., Eckman, R., Topiwala, N., Rodriguez-Alvarez, O., Cheek, D., and Hall, S.: The Stratospheric Aerosol and Gas Experiment (SAGE III) on the International Space Station (ISS) Mission, *Proc. SPIE Remote Sensing*, 9241, 924107, https://doi.org/10.1117/12.2073131, 2014.

Donovan, D. P., van Zadelhoff, G.-J., and Wang, P.: The EarthCARE lidar cloud and aerosol profile processor (A-PRO): the A-AER, A-EBD, A-TC, and A-ICE products, *Atmos. Meas. Tech.*, 17, 5301–5340, https://doi.org/10.5194/amt-17-5301-2024, 2024.

ESA Earth Online: ATLID Overview – Atmospheric Lidar, https://earth.esa.int/eogateway/instruments/atlid, last access: May 2026.

Feofilov, A. G., Chepfer, H., Noël, V., and Szczap, F.: Incorporating EarthCARE observations into a multi-lidar cloud climate record: the ATLID (Atmospheric Lidar) cloud climate product, *Atmos. Meas. Tech.*, 16, 3363–3390, https://doi.org/10.5194/amt-16-3363-2023, 2023.

Godin-Beekmann, S., Porteneuve, J., and Garnier, A.: Systematic DIAL lidar monitoring of the stratospheric ozone vertical distribution at Observatoire de Haute-Provence (43.92° N, 5.71° E), *J. Environ. Monitor.*, 5, 57–67, https://doi.org/10.1039/b211963e, 2003.

Haarig, M., Baars, H., König, L., Donovan, D., Ansmann, A., Khaykin, S., Ceolato, R., Cole, J., Gast, B., Floutsi, A. A., Heckmann, V. J., Hogan, R., Chantry, A., Marnas, F., van Zadelhoff, G.-J., and Wandinger, U.: The life cycle of a stratospheric smoke plume as seen from EarthCARE – tracking a plume from Canada to Europe, *Geophys. Res. Lett.*, 52, e2025GL119977, https://doi.org/10.1029/2025GL119977, 2026.

Kar, J., Lee, K.-P., Vaughan, M. A., Tackett, J. L., Trepte, C. R., Winker, D. M., Lucker, P. L., and Getzewich, B. J.: CALIPSO level 3 stratospheric aerosol profile product: version 1.00 algorithm description and initial assessment, *Atmos. Meas. Tech.*, 12, 6173–6191, https://doi.org/10.5194/amt-12-6173-2019, 2019.

Khaykin, S. M., Godin-Beekmann, S., Keckhut, P., Hauchecorne, A., Jumelet, J., Vernier, J.-P., Bourassa, A., Degenstein, D. A., Rieger, L. A., Bingen, C., Vanhellemont, F., Robert, C., DeLand, M., and Bhartia, P. K.: Variability and evolution of the midlatitude stratospheric aerosol budget from 22 years of ground-based lidar and satellite observations, *Atmos. Chem. Phys.*, 17, 1829–1845, https://doi.org/10.5194/acp-17-1829-2017, 2017.

Khaykin, S. M., Sicard, M., Leblanc, T., et al.: Global transport of stratospheric aerosol produced by the Ruang eruption from EarthCARE ATLID, limb-viewing satellites and ground-based lidar observations, *Atmos. Chem. Phys.*, 26, 607–622, https://doi.org/10.5194/acp-26-607-2026, 2026.

Knepp, T. N., Thomason, L., Roell, M., Damadeo, R., Leavor, K., Leblanc, T., Chouza, F., Khaykin, S., Godin-Beekmann, S., and Flittner, D.: Evaluation of a method for converting Stratospheric Aerosol and Gas Experiment (SAGE) extinction coefficients to backscatter coefficients for intercomparison with lidar observations, *Atmos. Meas. Tech.*, 13, 4261–4276, https://doi.org/10.5194/amt-13-4261-2020, 2020.

Kovilakam, M., Thomason, L. W., and Knepp, T.: SAGE III/ISS aerosol/cloud categorization and its impact on GloSSAC, *Atmos. Meas. Tech.*, 16, 2709–2730, https://doi.org/10.5194/amt-16-2709-2023, 2023.

Kremser, S., Thomason, L. W., von Hobe, M., et al.: Stratospheric aerosol – Observations, processes, and impact on climate, *Rev. Geophys.*, 54, 278–335, https://doi.org/10.1002/2015RG000511, 2016.

Leblanc, T., McDermid, I. S., and Raspey, R. A.: Long-term measurement trends at the JPL Table Mountain Facility, *Atmos. Meas. Tech.*, 5, 2917–2931, https://doi.org/10.5194/amt-5-2917-2012, 2012.

https://doi.org/10.5194/egusphere-2026-4358
Preprint. Discussion started: 29 July 2026
© Author(s) 2026. CC BY 4.0 License.

Leblanc, T., Sica, R. J., van Gijsel, J. A. E., Godin-Beekmann, S., Haefele, A., Trickl, T., Payen, G., and Gabarrot, F.: Proposed standardized definitions for vertical resolution and uncertainty in the NDACC lidar ozone and temperature algorithms – Part 1: Vertical resolution, *Atmos. Meas. Tech.*, 9, 4029–4049, https://doi.org/10.5194/amt-9-4029-2016, 2016a.

Leblanc, T., Sica, R. J., van Gijsel, J. A. E., Godin-Beekmann, S., Haefele, A., Trickl, T., Payen, G., and Liberti, G.: Proposed standardized definitions for vertical resolution and uncertainty in the NDACC lidar ozone and temperature algorithms – Part 2: Ozone DIAL uncertainty budget, *Atmos. Meas. Tech.*, 9, 4051–4078, https://doi.org/10.5194/amt-9-4051-2016, 2016b.

NDACC: Lidar Instruments – Network for the Detection of Atmospheric Composition Change, https://ndacc.larc.nasa.gov/instruments/lidar, last access: May 2026.

Thomason, L. W., Kovilakam, M., Schmidt, A., von Savigny, C., Deshler, T., and Rieger, L.: Quantifying SAGE II (1984–2005) and SAGE III/ISS (2017–2022) stratospheric aerosol measurements, *NASA Technical Reports Server*, https://ntrs.nasa.gov/citations/20230014708, 2023.

van Zadelhoff, G.-J., Barker, H. W., Baudrez, E., et al.: The EarthCARE mission: science data processing chain overview, *Atmos. Meas. Tech.*, 17, 839–862, https://doi.org/10.5194/amt-17-839-2024, 2024.

Wehr, T., Kubota, T., Tzeremes, G., et al.: The EarthCARE mission – science and system overview, *Atmos. Meas. Tech.*, 16, 3581–3615, https://doi.org/10.5194/amt-16-3581-2023, 2023.